A&A 466, 675–682 (2007)
DOI: 10.1051/0004-6361:20066639
© ESO 2007

Astronomy & Astrophysics

Variations of the ultraviolet resonance lines of the B2 IV-V star ζ Cassiopeiae

M. A. Smith[1,⋆] and D. A. Bohlender[2]

[1] Department of Physics, Catholic University of America, Washington, DC 20064, USA
e-mail: msmith@stsci.edu
[2] National Research Council of Canada, Herzberg Institute of Astrophysics, 5071 W. Saanich Rd., Victoria, BC V9E 2E7, Canada

Received 26 October 2006 / Accepted 7 February 2007

ABSTRACT

Recently Neiner et al. reported that the B2 IV-V star ζ Cas contains a weak magnetic field which varies on the same 5.37 day period found from the modulations of its N V, C IV, and Si IV UV resonance lines. We have studied the time variable properties of the same resonance lines in greater detail to determine the physical characteristics of the magnetospheric structure responsible for them. In our formulation this structure takes the form of an axisymmetric "disk" similar to those around magnetic He-strong Bp stars. This structure corotates with the star, covering greater or lesser amounts of its area during its transit. ζ Cas offers a special case because we observe it from a low inclination and yet its magnetic axis is substantially inclined to the rotation axis. The equivalent width-phase curves show a flat maximum for half the cycle, indicating that the disk is extended out of the plane, extends to the star's surface in the magnetic plane, or both. Synthetic spectra of the line profiles during the maximum and minimum occultation phases can be best reconciled with a disk geometry in which the resonance lines are formed at a closed outer edge and along a thin outer layer. We speculate that observed weak redshifted emission is formed in "auroral caps" located near the magnetic poles of the star. We argue that this results from shocks of stagnated wind material returning to the star and shocking against the outflowing wind.

Key words. stars: individual: ζ Cassiopeiae – magnetic fields – stars: circumstellar matter – stars: winds, outflows – stars: early-type – ultraviolet: stars

1. Introduction

Fully twenty years ago Grady et al. (1987) and Sonneborn et al. (1987) reported that the UV resonance lines of the sharp-lined B2 IV-V star ζ Cassiopeiae (HD 3360; $V = 3.67$) are variable. Interest in this star has been rekindled recently by the report by Neiner et al. (2003; hereafter N03) that this star has a dipolar magnetic field of $B_z \approx 335$ G varying by ±28 G with a period of 5.37 days. The resonance lines of N V, C IV, and Si IV show variations with the same period. N03 also report a nitrogen abundance enhancement and a marginal helium overabundance ([He] = 0.11 ± 0.06 dex). These characteristics make ζ Cas a likely weak member of the magnetic He-strong Bp stars. We note for completeness that small-amplitude nonradial pulsations are excited on this semi-evolved star's surface (e.g., Sadsaoud et al. 1994).

It is generally accepted that magnetic Bp stars contain fossil dipolar magnetic fields that are randomly oriented with respect to the rotational axes. Many authors (e.g., Shore 1987; Shore & Brown 1990; Babel & Montmerle 1997a,b) have attributed the time-modulated UV resonance line variations to the channeling of radiative winds from their magnetic poles to their equators. Because ionized particles cannot cross magnetic field lines, the global stellar fields play a key role in the wind outflows. Although the particles emerging from the magnetic poles can freely accelerate, wind flows are prevented from crossing transverse stellar field lines in the equatorial zones and are suppressed. Moreover, the field lines emanating from the stellar magnetic poles channel the escaping wind toward the magnetic plane. Here they collide with wind streams coming from the opposite magnetic hemisphere. This produces a shock that overionizes particles which then reionize and deexcite and emit resonance line radiation. The resonance line radiation is then scattered through the confined structure, allowing the observer to see an array of absorption and emission components as the corotating disk/shock complex corotates around the star. Many of the cooled particles settle toward the plane to form a confined "disk". Interior to the magnetospheric structure, a sector of this disk transits in front of the star and occults part of the star's projected area and causes excess absorption in low-excitation lines of iron group ions. In Bp stars with extensive disks, the absorption from this "iron curtain" forest is made visible by their composite effect in high resolution spectra obtained by the *International Ultraviolet Explorer (IUE)* (Smith & Groote 2001; hereafter SG01) and in high-level Balmer lines (Groote & Hunger 1976).

In the hydrodynamic formulation of this process by Babel and coworkers, a shock develops where the disk particle pressure equals the wind's energy density. Important refinements have been added to the Babel picture by ud-Doula and collaborators by considering the relative influences of other forces on particles along the flow. We summarize several effects they can have on the disk structure:

– Ud-Doula & Owocki (2002; hereafter uO02) found that the confinement of the wind by the star's magnetic field is given by a ratio "η_*" of surface magnetic to wind energy densities. These authors also found that the weight of the wind particles produces a feedback on the field lines in which the stagnated

⋆ *Present address*: Space Telescope Science Institute, 3700 San Martin Dr., Baltimore, MD 21218, USA.

Article published by EDP Sciences and available at http://www.aanda.org or http://dx.doi.org/10.1051/0004-6361:20066639

wind drags the lines of force inward along the equatorial plane. In some circumstances, the particles may collapse the field lines back into the star's equatorial regions. More typically, condensations form chaotically as snake-like blobs. These structures fall back toward the star, out of the plane and along the lines of force. UO02 suggested that this sequence of events is responsible for the UV emission lines in Bp star spectra. Gagné et al. (2005; G05) developed this idea to explain emission from the hot Bp analog θ^1 Ori C. A byproduct of this picture is that matter does not fall straight inward along the magnetic plane to the star's surface. The effect is to produce a discrete inner edge to the disk. Interior to this point there is effectively no matter.

- Refinements in the picture have shown the importance of angular momentum conservation and the tendency of particles to accumulate in magnetospheric regions of minimum potential energy (Preuss 2004; Townsend & Owocki 2005). These forces can cause the disk to warp for a range of magnetic inclinations and also permit the particles to accumulate at the intersections of the magnetic and rotational equators and in other areas outside the planes. The effect of these accumulations is that disks of rapidly rotating Bp stars may show departures from coplanarity and axisymmetry.
- Ud-Doula et al. (2006, u06) found that lines of force near the Alfvén point of rotating stars are stretched outward by the centrifugal force. At irregular intervals, the field lines severe, and disk material "breaks out" through the Alfvén point at the equator. The heating of material by this process may be the source of X-ray flares, such as observed in the prototypical magnetic Bp star σ Ori E (e.g., Groote & Schmitt 2004).
- Including post-shock cooling energetics into quasi-equilibrium magnetic wind models leads to the prediction of a range of temperatures from 10^8 K to 10^6 K or less (Tonneson et al. 2002, G05). This shock region is confined to a broad zone just inside the Alfvén radius. Interior to this zone, wind particles are not accelerated to high enough velocities to produce "superions" and resonance line radiation.

For relatively slowly rotating, weakly magnetic stars like ζ Cas some of these processes are not expected to be important. An important modification of the Babel model is that the wind detritus returns to the star along lines of force where it collides with high latitude wind streams.

2. Methodology

2.1. Reduction of ultraviolet resonance lines

The ultraviolet spectra for this program included the wavelength regions surrounding the N V, C IV, Si IV, and Al III resonance lines and recorded on *IUE* echellograms with the Short Wavelength Prime (SWP) camera. These data were obtained from the MAST archives[1]. We found 106 spectra, all obtained between 1979 and 1995 and all observed through the *IUE's* large aperture, were suitable for analysis. We then computed "equivalent width (EW) indices" by ratioing the fluxes within the line edges with fluxes of other wavelengths in the order (see SG01). Spectra for phase ranges given in Sect. 3.1 were selected, "conditioned", and coadded by carrying out the following operations: (1) cross-correlating them to remove apparent wavelength shifts, (2) forcing them to a common continuum slope across the order, and (3) weighting the individual spectra according to the mean fluctuation from pixels of neighboring resolution elements. This weighting was accomplished by evaluating the internal spectrum rms noise (assumed to be the median value of the absolute value of the fluctuations of pixels in each neighboring resolution element, i.e., every 3rd pixel). The principal work in this paper concerns the analysis of pairs of coadded resonance line spectra obtained at phases near the passage of the South magnetic pole across the star's central meridian (following N03, taken to be $\phi = 0.0$), and approximately 0.5 cycles later, i.e., when these lines exhibited minimum and maximum absorption, respectively. We quantified the variations of these line profiles in our first figure by measuring a dimensionless "equivalent width index" rather than a true equivalent width (EW) in Angstrom units. Our index is defined as the ratio of all fluxes within a designated window across the profile to all fluxes outside them in the echelle order containing them. Our indices are proportional to a true equivalent width but do not rely upon inaccurate placements of the local continua. For the case of ζ Cas, the windows were taken to be the instrumentally broadened photospheric line profile, or ±0.8 Å for most resonance lines (±0.5 Å for N V).

2.2. Optical data

In an attempt to search for variations in high-level Balmer lines from the variable occultation of the star by the disk, we obtained 31 spectra with the 1.85 m telescope of the Dominion Astrophysical Observatory during 2005, December 16, 2006 February 14–16 and March 8. We used the f/5 Cassegrain spectrograph and fed the light to a CCD detector by means of an image slicer. The resulting spectra have a dispersion of 10 Å mm^{-1}, a resolution of about 16 400, and cover the wavelength region $\lambda\lambda$3610–3880. These data gave a null result, as reported below.

2.3. Spectral synthesis computations

To perform the analysis of the *IUE* spectra, we utilized a suite of programs written by I. Hubeny and collaborators and non-LTE solar abundance BSTAR models (Lanz & Hubeny 2006). The first of these, *synspec,* is a photospheric line synthesis program (Hubeny et al. 1994) used for the reference photospheric profiles. This program permits one to modify assumed chemical abundances in the atmosphere. Indeed, the strengths of the Fe III lines in the *IUE* spectrum suggested an iron abundance of $\frac{1}{3}$ the solar value, assuming a photospheric microturbulence $\xi_t = 2$ km s^{-1}. We also used *synspec* to convolve the photospheric lines with functions approximating the instrumental and rotational broadenings for the instrument and the star. The spectroscopic resolution of *IUE* high-dispersion spectra is about 13 000 and the the star's rotational broadening ($v \sin i$ = 17 km s^{-1}) are comparable. We computed the synthetic spectra in steps of 0.01 Å.

Our goal in this analysis is to assess the effects of the magnetospheric disk on the UV resonance line spectrum as the disk moves across the surface of ζ Cas, alternately occulting greater or lesser areas of the star in its circuit. To simulate the absorption and emission signatures of the disk on the spectrum, we used the radiative transfer program *circus* (Hubeny & Heap 1996; Hubeny & Lanz 1996). This program computes strengths of absorption or emission components of lines in a circumstellar medium from user-input quantities such as disk temperature, column density, areal coverage factor (the portion of the disk that

[1] Multi-Mission Archive at Space Telescope Science Institute, in contract to NASA.

passes in front of the star), and microturbulent velocity. *Circus* combines this contribution with the *synspec*-computed spectrum of the photosphere. In its solution of the radiative transfer, *circus* calculates line emissions and absorptions separately along a line of sight. The emission is computed according to the assumption of LTE for an input disk temperature $T_{\rm disk}$. Because the "absorption" of resonance lines is actually due to scattering, it can be handled by turning off a flag in the program that computes the emissivity coefficient in the radiative transport equation. The result is that the background flux of the star is affected only by the absorption coefficient. The ability of handling the line transfer in this way permits one to treat absorptions and emissions simultaneously or separately in different circumstellar structures. *Circus* can accommodate three separate "clouds". In the present analysis, we found it necessary to include two cloud structures, one for the excess absorptions of the resonance lines and a second for the emission components. The program allows us to input different radial velocities and temperatures that might be useful in testing whether different diagnostics are formed in separate regions, allowing an assessment of whether they might arise in different volumes. As in the work described by SG01 and Smith et al. (2006; hereafter S06), we have assumed the clouds to be homogeneous in all properties. However, the MHD studies described above suggest this may well be an oversimplification.

Among other input parameters are the disk's volume density and microturbulent velocity ξ. Our results were insensitive to the values chosen for either of them. The volume density enters only indirectly (and insensitively) through the gas ionization equilibrium. Our trial input density, $\sim 10^{12}$ cm^{-3}, is the order of magnitude SG01 determined for hot Bp star disks and is also the peak value determined by the MHD simulations. Except for the absorptions of the primary resonance lines (C IV, Si IV) the overwhelming majority of the UV metal lines in our computations are optically thin. Since the spectral signatures then scale as the volume of absorbers, a degeneracy arises between two geometrical factors of the disk: its area and column length along the observer's line of sight.

The final ingredient of our models is the treatment of line of sight velocities. Because the magnetosphere co-rotates over the star's surface, no differential velocities exist along the line of sight to the star during occultation. Moreover, the Doppler shift of the disk absorbers is matched by the velocity of the star area behind them. SG01 found that turbulent velocities in the range of 0 – 20 km s^{-1} can be offset by changes in the assumed metallicity in the disk because the lines are optically thin. These authors also found a broadening of the Al III and N V resonance lines of about 25 km s^{-1} and 50 km s^{-1}, respectively, at phases near maximum occultation. The *circus* models were computed with the same underabundant iron abundance as determined for the photosphere. We used solar abundances of C, Si, and Al, but an overabundance [N] = 0.4 dex (N03), all with a ξ = 20 km s^{-1}.

2.4. Relevant rotational and magnetic parameters

In our analysis we have assumed the physical parameters of ζ Cas determined by N03. These include the redetermination of the star's effective temperature, near 21 000 K and a logarithmic surface gravity of about 3.8. Therefore, we have chosen the (21 000, 4) model in the BSTAR grid as input to our *synspec* computations. At the surface of the star, small amplitude nonradial pulsations are present (N03), but we ignore them in this discussion. Given a period of 5.37 days and the star's $v_{\rm e} \sin i$ = 17 km s^{-1}, the inferred equatorial rotational velocity, $v_{\rm e}$ = 55 km s^{-1}, is also well determined: ζ Cas is a moderately rotating B star. N03 give a rotational obliquity angle of $i = 18 \pm 4°$. From i and attributes of the magnetic phase, curve N03 derive a magnetic obliquity angle, $\beta = 79 \pm 3°$.

The rotational phase zero ϕ is taken as the stellar longitude containing the negative poles in the visible hemisphere. Then the viewing angle α can be written as:

$$\cos\,\alpha = \sin\,\beta\,\cos\,\phi\,\sin\,i + \cos\,\beta\,\cos\,i, \quad (1)$$

one sees that for small i and large β that the viewing angle changes little through the rotation cycle. Consequently, we can expect only small changes in the absorption coverage factors of the disk in front of the star.

The relation for the wind magnetic confinement parameter η_* is given by uO05 as the ratio of magnetic to kinetic energies, namely as:

$$\eta_* = B_z^2 R_*^2/(\dot{M} v_\infty). \quad (2)$$

Here the symbols refer the the polar magnetic flux B_z, stellar radius R_*, and mass loss rate $\dot{M}$, and the wind velocity at infinity v_∞. One is somewhat handicapped in evaluating η_* because no modeling has been performed of ζ Cas's wind attributes. Therefore, we will take mean values for a B2 V star: $\dot{M} = 3 \times 10^{-10}\ M_\odot$ yr^{-1} (Snow 1981). We estimate that v_∞ = 800 km s^{-1} from the line profiles and R_* = 5.9 $R_\odot$ from N03. Then, $\eta_* \sim 10^3$. This is a large value but still about 10^{-4} times the value found for σ Ori E and 36 Lyn (S06). However, the mass loss rate for ζ Cas may be anomalously high. For example, Slettebak (1994) found that the combined equivalent widths for the the C IV and Si IV doublets for this star are 2.40 Å and 3.59 Å, respectively, whereas the corresponding values for an average B2 V star are 1.35 Å and 2.85 Å. If this is the case, then η_* should be taken as an upper limit. Finally, we can estimate the location of the Alfvén radius from the approximation $R_{\rm Alf} \approx \eta^{\frac{1}{4}}$. Thus, $R_{\rm Alf,*} \approx 5\ R_*$.

3. Results

3.1. The UV resonance line variations with phase

N03 have determined a period of 3.57045 ± 0.00008 days from the variations of the C IV, Si IV, and N V resonance lines. To check this value, we applied the PDM period-finding algorithm (Stellingwerf 1978) to EW indices extracted from the resonance lines as defined above. These extractions were done in the inner ±0.5 Å of the N V lines and inner ±0.9 Å of the C IV and Si IV lines. We ordered these values by time and and found a value of 3.57038 ± 0.0001 days, thereby verifying the N03 value. We used this period and the N03 zero point (ϕ = 0 at HJD 2 446 879.889) to compute rotational phases. Figure 1 exhibits the absorptions (EW index) folded around this period, but we have rescaled them so that each exhibits the same fractional variation (this rendition artificially increases the apparent noise in the N V curve). Note the Fig. 1 minimum centered at phase 0.0. Also, as previously pointed out by N03, one may discern a hint of a secondary minimum on the broader maximum at $\phi \approx 0.50$, but we are not convinced that it is statistically significant since this feature does not appear in the Si IV or N V curves. Finally, we point out that the shapes of the absorption-phase curves are indistinguishable from one another. This is surprising because, as noted below, the decreased absorptions they represent occur for both optically thick and thin lines.

To reconnoiter the modulation of the line strengths with phase, we first grouped over 20 spectra each into EW-minimum

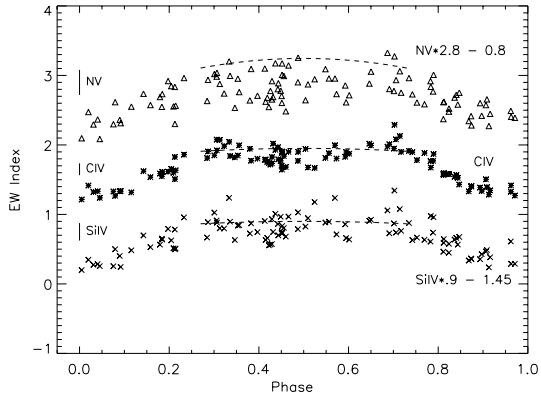

Fig. 1. Variation of line strength indices for the UV resonance doublets of N V, Si IV, and C IV with phase in the spectrum of ζ Cas. Scaling factors are applied to show the same apparent amplitude; vertical shifts are made for clarity. Approximate measurement errors are indicated. The dashed, tapered line shows the assumed limiting absorption relation (see text).

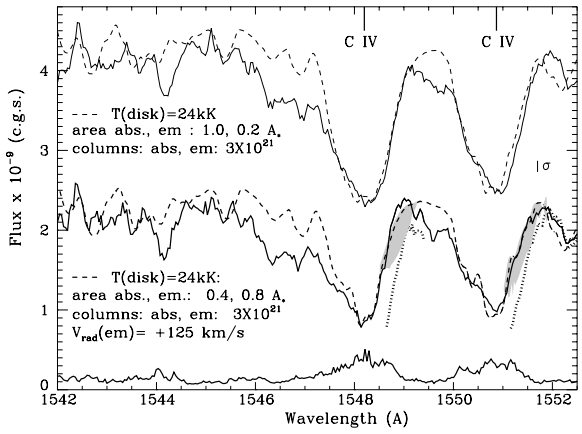

Fig. 2. Maximum (upper) and minimum absorption lines of the C IV doublet of ζ Cas fit with synthetic spectra (dashed lines). Fitting parameters are indicated (see Table 1). The shaded area denotes the emission component determined in the models; the dotted line in the lower plot repeats the maximum absorption profile in this same wavelength range for comparison. The blue wing absorption of the C IV lines is due to the (unmodeled) wind contribution. The rms spectra is also shown.

and EW-maximum phase bins corresponding to ϕ = 0.89–0.11 and 0.30–0.70, respectively, and computed mean spectra from these groups. The results are exhibited as thick solid lines in Figs. 2 and 3 for the wavelength regions surrounding the C IV and N V doublets, respectively. Minimum and maximum spectra were also computed for the Si IV lines. The line profiles of the spectra are different in that those for the former phases exhibit smaller absorptions and generally steeper red wings. Part of the asymmetry in the wings is due to the influence of the winds. As for other Bp stars and θ^1 Ori C (Smith & Fullerton 2005), this wind is focused by the magnetic field and streams outward preferentially at low magnetic latitudes. Since the wind escapes from regions outside this disk, we do not model it in this work. The red shoulders of the profiles at these times are steep with respect to our computed photospheric profiles, and we attribute this to an incipient redshifted emission. We attribute the strengthening of the spectra to increased blocking of the stellar flux by the intervening disk. Our modeling of absorptions and emissions

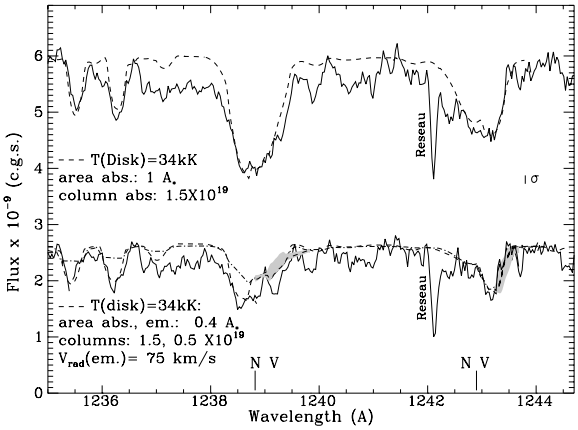

Fig. 3. Maximum (upper) and minimum absorption in the N V doublet lines of ζ Cas fit with synthetic spectra (dashed lines). Fitting parameters are indicated (see also Table 1). Vestigial emission (shaded area) in λ1242 is suggested in our model.

proceeded with these assumptions, and we defer the discussion of results to the next section.

3.2. Quantitative analysis of the C IV and N V resonance lines

3.2.1. The maximum and minimum absorption spectra

We have described a picture in which wind particles escaping the magnetic poles of a Bp star shock when they impact particles near the magnetic equator that have formerly settled to form a cooled "disk". The phase-dependent absorptions of key ultraviolet lines validates this basic picture for ζ Cas. The morphology of the resonance lines shown is replicated within the errors by less excited resonance lines of Al III and C II, thereby providing evidence that the structure is a confined cool disk. However, we were not able to estimate the disk temperature from ratios of iron line absorptions because the available Fe II lines are too weak to show variations. Even so, if we assume the relation for the cool disk ionization temperature $T_{\rm disk} \approx 0.6\,T_{\rm eff}$, as found in the Bp stars studied by SG01 and S06, we obtain a value $T_{\rm disk}$ = 12 000 K. Assuming this temperature and, in the absence of information about the extent of the coverage of the star by the cool disk component during the occultation phase, we find from *circus* modeling of the small variations of the Al III λ1855–62 and the C II $\lambda\lambda$1335-6 multiplets that the hydrogen column densities of the occulting disk are $1{\times}10^{18}$ cm^{-2}, assuming ξ = 20 km s^{-1}, and 2×10^{18} cm^{-2}, assuming ξ = 10 km s^{-1}. We take these as convenient lower and upper estimates.

We note that after reducing our DAO spectra of the high-level (H8–H13) Balmer lines and plotting the equivalent widths with phase, we were unable to find statistically significant variations in them. From our the measurement errors, ±0.6% per line, this undetectability translates to a column density of $\sim 4 \times 10^{20}$ cm^{-2}, according to our *circus* simulations, and assuming a $T_{\rm disk}$ = 12 000 K. Since this limit is a few hundred times higher than the limits imposed by the Al III and C II variations just above, it does not add information to the disk analysis.

The resonance line variations in the two figures bring out two interesting characteristics. First, notice that the rms spectra in the C IV line figure show that the profile activity is confined to roughly ±100 km s^{-1} from line center. However, the wind-depressed blue wings undergo no activity through the cycle.

Table 1. Derived columns, areal coverages, and radial velocities (km s^{-1}) inferred from UV resonance lines.

N V lines	(ξ = 75 km s^{-1}):							
$T_{\rm disk}$	Col. density		Fractional	Area	Vel.	Vel.	$\tau_{\rm line}$	$\tau_{\rm line}$
	(Abs)	(Emis)	(Abs)	(Emis)	(Abs)	(Emis)	(Abs)	(Emis)
34 000	1.5×10^{19}	–	1.0	0.0	0	–	0.3	–
34 000	1.5×10^{19}	5×10^{18}	0.4	0.4:	0	+75	0.3	0.1
28 000	3×10^{21}	–	1.0	0.0	0	–	0.6	–
28 000	3×10^{21}	3×10^{21}	0.4	0.4:	0	+50	0.6	0.6
C IV lines	(ξ = 90 km s^{-1}):							
$T_{\rm disk}$	Col. density		Fractional	Area	Vel.	Vel.	$\tau_{\rm line}$	$\tau_{\rm line}$
	(Abs)	(Emis)	(Abs)	(Emis)	(Abs)	(Emis)	(Abs)	(Emis)
24 000	3×10^{21}	–	1.0	0.2	0	–	15	–
24 000	3×10^{21}	3×10^{21}	0.4	0.8	0	+125	5	5
20 000	3.5×10^{19}	–	1.0	0.0	0	–	40	–
20 000	1.7×10^{17}	1.7×10^{17}	0.4	1.0	0	+125	0.2	0.2
Si IV λ1403	(ξ = 75):							
$T_{\rm disk}$	Col. density		Fractional	Area	Vel.	Vel.	$\tau_{\rm line}$	$\tau_{\rm line}$
	(Abs)	(Emis)	(Abs)	(Emis)	(Abs)	(Emis)	(Abs)	(Emis)
22 000	5×10^{18}	–	1.0	0.0	0	–	2	–
22 000	5×10^{18}	5×10^{18}	1.0	2.0	+25	+50	2	2
18 000	3×10^{18}	–	1.0	0.0	0	–	1.5	–
18 000	3×10^{18}	3×10^{18}	1.0	6.5	+25	+50	1.5	1.5

Similar to the resonance lines of other Bp stars, the rms spectral amplitudes peak to the red of the line centers. Inspection shows that this is caused primarily by steepenings of the red shoulder of the lines in observations obtained in the EW-minimum phases. According to the line fittings discussed below, these shoulders cannot be fit by photospheric spectra or disk absorption spectra. Rather, we believe these are incipient emissions corresponding to the more pronounced emissions observed in many Bp star spectra. Another characteristic brought out in these plots is that the doublet ratios of these activities are 1.2 and 1.0 ± 0.2 for the C IV and Si IV (not shown) lines, respectively. The ratio for the N V lines is 2.5 ± 0.4. From these ratios we can see that the circumstellar media in which the "disk" component of C IV and Si IV are formed are optically thick while the N V lines optically thin, much like their photospheric components.

3.2.2. Fitting of the resonance doublets

In our line profile fitting we found that an important diagnostic is the line optical depths. Because the optical depths of our models are typically within an order of magnitude of unity, we were able to use them to estimate the optical depths of the disk columns and ultimately to set limits on the range of the disk temperature $T_{\rm disk}$. These values are represented in the table discussed below.

Our initial attempts to model the minimum and maximum EW spectra in Figs. 2 and 3 used input *circus* parameters for a single homogeneous absorbing and emitting circumstellar "cloud". The models assume a disk temperature $T_{\rm disk}$, which for simplicity we have assumed to be the same value. This group of models failed to give satisfactory fits. Although there were several problems with the fits, the most important was the inability of the models to produce enough absorption to fit the EW variations. This problem was accentuated by the constraint that the change of coverage of the star must be incomplete because of the low inclination of the star. Investigating this failure in more detail, we found that the poor fits extended over a significant wavelength range. For this reason, we were forced to consider *circus* models fit with two homogeneous clouds with different properties, especially radial velocity. These models were successful, but only when we increased the microturbulence ξ to 75–90 km s^{-1}. We note by contrast that high cloud macroturbulences merely smear the computed excess absorptions and emissions. They do not strengthen them, as is required by the observations.

We were not led immediately to our best fits with the two-cloud description. Moreover, those we have selected for representation are those obtained only for one possible disk temperature among the range of $T_{\rm disk}$ values. One of the most important fitting parameters, the temperature implied by fits to the emission components, $T_{\rm emis}$, is not uniquely determined. For the C IV line fitting, the upper limit on $T_{\rm emis}$, 26 000 K, was set by the decreased optical depths in the line that led to different and contradictory absorbing cloud areas or columns for the two doublet components. The lower limit of 16 000 K was set by the appearance of nearby Fe II lines in the computed models, which are not present in the observations. For the N V lines a low temperature limit of 26 000 K was again set by the absence of a predicted iron line (Fe III 1243.4 Å). The column density required for fitting the N V lines rapidly decreases to the values found for the C IV fittings, and we consider this the most likely result.

Table 1 shows the results of best two-cloud models for the maximum and minimum EW profiles of the N V, C IV and Si IV doublets, that is for observations obtained near mid-transit (maximum occultation) phases and those for half a cycle later, respectively. An example of a model for the C IV and N V doublets is shown in Figs. 2 and 3 as a dashed line. Annotations give pertinent model fitting parameters. Shadings denote the modeled incipient emissions. In the table we give both "high" and "low" $T_{\rm disk}$ values, as discussed above. In each case we give modeling parameters for fits to the maximum EW and minimum EW line in the upper and lower lines of each double row entry. In the table we give several key fitting parameters, including the $T_{\rm disk}$, column density, areal coverage, radial velocity, and central optical depth of the stronger doublet member. Errors were estimated by repeating our models with single parameters changed by varying degrees and comparing the resulting differences in the equivalent widths with 2σ changes in the line profiles within the same

wavelength window from the rms errors in the *IUE* spectra. The latter was accomplishing using a Monte Carlo approach to compute the fluctuations as described in Smith (2006). These errors led to the following estimated 2σ errors in our table: ± 15 km s^{-1} in microturbulence ξ, $\pm 20\%$ in fractional areal coverage for C IV and Si IV, and $\pm 50\%$ in the column densities. The errors for the latter two quantities are $\pm 100\%$ for the N V doublet. Inspection of this table brings out the following points:

- Unlike the cases of *equator-on* Bp stars with large β angles, occultation of some part of the stellar disk occurs to one extent or another at all rotational phases. This is expected for star-disk systems with a small i. This circumstance also hints that the disk is either extended in height (perpendicular to the plane) or extends inward to reach the star in the magnetic plane.
- The column density and hence volume ratio of shocked gas in which the resonance line emission and scattering occurs is several times that of the column density inferred from the less excited C II and Al III ions. This result contrasts with the SG01 finding for other Bp stars, where the ratios were comparable. This indicates that the ratios of the volumes can be quite different among Bp stars and opens the door to the possibility that they are not cospatial.
- An important parameter in our fittings was the radial velocity of the emission component – typically $+50$–125 ± 20 km s^{-1}. Its errors were estimated by a comparison of values found for the doublet members.
- The large ξ values for Bp disk absorptions and emissions is typically high (SG01, S06), and we cannot verify that it is a true microturbulence. Irrespective of data quality limitations, there is an intrinsic interpretational ambiguity between geometries that imply a large ξ in a single structure and multi-columns each with smaller ξ values and separated in radial velocity. Such a contrivance would both broaden and strengthen the excess absorptions and emissions.

4. Interpretation

In S06 we described a computer program written to describe the varying excess absorptions of an optically thick resonance line as a co-rotating disk shaped like a cylinder transits across the star. The line is assumed to be optically thick, the absorption of flux from the obscured region of the star is total. Then, one may express the occulted area of the star in terms of the excess absorption measured.

One can manipulate input parameters representing the dimensions of the disk to fit observed phase absorption curves. For the case of ζ Cas, the curves in Fig. 1 show that the absorption curves are essentially *flat* out to $\pm\frac{1}{4}$ cycles around maximum occultation phase, $\phi \approx 0.50$. Unfortunately, flat absorption phase curves give information only on the limits of ratios of dimensions[2]. This problem is aggravated by the low S/N of *IUE* data, which makes it difficult to map the progress of the disk viewed at a low i. However, we may still investigate the general character of the disk cylinder shape if we estimate a minimum taper in the curves (5% of the maximum excess absorption out to $\phi = 0.25$ and 0.75) that might be hidden in the noise of the absorption curves. This taper is shown in Fig. 1 as a dashed line.

Applying this criterion and the i and β values for ζ Cas, we adopt an outer disk radius $r_{\rm outer} = R_{\rm Alf}$, and we can ask, what is the interdependence between the height (measured parallel to the rotational axis) and the thickness of the disk in the radial direction, $r_{\rm outer} - r_{\rm inner}$? According to our models and our taper criterion, a disk extending in to the star's surface along the magnetic plane can protrude no further than 3.2 R_* from the central plane. For a second case for which the disk has an inner radius of 3 R_* (i.e., an evacuation of the inner 50% of the disk), our models produce a similarly tapered phase if the disk extends $\geq$3.0 R_* out of the magnetic plane. For the cylindrical model we have adopted there is a degeneracy between these dimensions – we have little leverage in determining where an inner disk edge lies. More importantly than this, the implication from the cylindrical model representation is that the disk extends to surprisingly large distances from the central plane. There is no indication that disks of other Bp stars extend out of the plane to similar distances. It seems more likely that our assumed disk geometry is in conflict with fitting difficulties that are aggravated for star-disk systems observed from a low inclination.

Although the concern just raised over our disk geometry arises from the combination of high β and low i for the ζ Cas case, the resonance line absorption curves of stars having high β and i values pose their own interpretational dilemmas. The most significant of these is a fact noted by SG01 for those systems for which the observer's observer's line of sight runs through the magnetic plane. In these cases, the complete occultation of the star disk in optically thick resonance lines presents the physical problem of how superions responsible for the line scattering can be distributed throughout the cylinder. How can such ions be excited in the middle of an optically thick medium? This puzzle can be solved if, as predicted in the MHD models of ud-Doula and coworkers, the disk is pinched off at the Alfvén radius in the equator by the confluence of collimated wind streams. Exterior to this point the field lines curve out and run parallel to the magnetic equator. Then, an external observer at infinity viewing the system in the magnetic plane sees the emission from excited superions along this (thin) geometric boundary.

A third difficulty offered for the cylindrical geometry, again evident for the ζ Cas case, is that the absorptions should scale differently for optically thick and thin lines as the disk moves off the limb of the star. The excess absorptions of these two groups of lines should scale differently – as the area and the volume of the occulting disk, respectively. In contrast, we find that when the curves in Fig. 1 are overplotted, their morphology is indistinguishable for the two types of lines. This difficulty is inherent for any "solid" disk geometry. It can be avoided if the disk opacity is confined to a thin outer region having similar depth ranges of formation for these lines. This circumstance is permitted if the volumes of excited ions are confined to the outer regions of the disk.

In Fig. 4 we suggest a revised geometry in which the outer disk edge, representing the wind-disk shock, tapers toward the equator and thus takes the general shape of an oblate spheroid[3]. We envisage that the excited "super-ions" are formed in a thin outer shell of this structure. The column and volume densities can then be made consistent if the absorption column lengths, as

[2] Although we have discounted the statistical significance of a secondary dip in the phase curves, if they are real it could be interpreted as a *dearth* of overionized particles like C^{3+} in zones over the rotational poles. This would agree with uO02's expectations that the particles exert a feedback on the magnetic field and drag them away from zones of low angular momentum. Evidence for this avoidance would be visible only for rotating magnetic stars observed at low inclinations.

[3] Rather than an oblate spheroid, the circumstellar disk region could take on just as well a negative curvature, coming to a cusp at the equator. The important point in our picture is not the exact shape but that it be closed at the equator and have about the height and radii we determine.

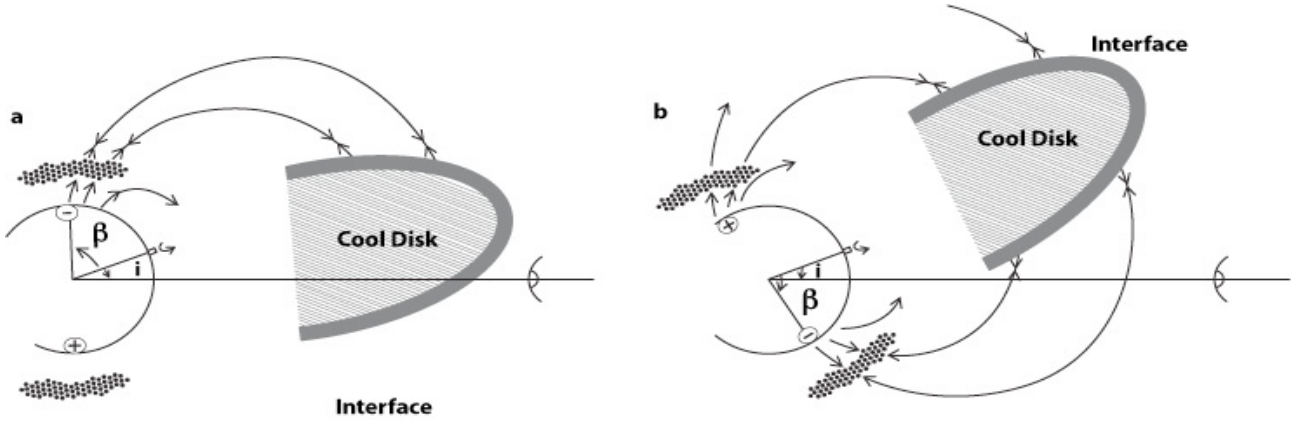

Fig. 4. The geometry at the times of maximum ($\phi = 0.5$) and minimum ($\phi = 0$) absorptions of the resonance lines of ζ Cas in panels **a)** and **b)**, respectively. The observer is to the right. The angles $i = 18°$ and $\beta = 79°$ are taken from N03. Low-excitation line absorptions are formed in the optically-thin disk interior. Closed at the outer end, the disk is centered around the magnetic equatorial plane and taken to be an oblate spheroid. The outer edge of the disk is heated by impacts from the high velocity wind and includes superions responsible for the resonance line absorptions. Net redshifted emissions are produced in an "auroral cap" shown as a dotted region over the magnetic poles (at ~11 and ~5 o'clock positions).

in Table 1, refer to a common shell thickness. For densities predicted by uO02 and column lengths in Table 1, the shell thickness to $\tau = 1$ is then only of the order 10^3 km. Since the resonance lines are formed in a skin around a cool transparent disk, there need be no relation between their column densities and those inferred from the Al III and C II lines.

The regions where the resonance line emissions arise likewise should be reconsidered, as they cannot be understood as the result of the interaction of the wind and the edge of a dense disk. Consider first that for the Bp stars with dense, extensive disks investigated by SG01, the emissions can be present at all phases. The SG01 picture was that the resonance lines exhibit emission preferentially at those phases when the disk is viewed nearly face-on in the plane of the sky. A problem with this geometry is the positive radial velocity of the emissions. In contrast to SG01, we now believe the redshifts do not arise from the impact of the wind particles against the disk interface. Such interactions would produce emissions, but they are centered in the rest frame of the star.

A second problem is that the *ratios* of volumes computed from these lines' emissions and excess absorptions can be quite diverse among Bp stars. However, they should be approximately equal if the contributions in the same disk volumes arise from scatterings. These scatterings are conserved when integrated over all lines of sight.

These issues can be addressed by positing that the absorptions and most of the emissions of UV resonance lines are formed in different places. Our revised geometrical picture harkens back to the results of two-dimensional MHD models of the emission complex surrounding θ^1 Ori C discussed by uO02 and G05. Recall that these models predict that infall condensations fall back into the outflowing wind. Indeed, the collision of these two structures will produce redshifted emission in the external reference frame because the center of mass is dominated by the falling blobs. These emissions are visible mainly over a narrow range of phases because the projected shock areas modulate with viewing angle. For θ^1 Ori C the projected radial velocity in the UV and X-ray resonance line is observed to be $\gtrsim$100 km s^{-1} (Smith & Fullerton 2005, G05).

We now ask what would be outcome of this same process if the wind were weaker? We speculate that the answer begins with the fact that because the lower efflux would provide less resistance to the infall, the shock front where the pressures equalize will lie closer to the star. This shock point will then occur where the dense fallback blobs have accelerated to a higher velocity, while the wind outflow, intercepting them from the opposite direction, has only begun to accelerate. For a sufficiently weak wind (and similar η_*) the shock front should then describe an arc-like "auroral" cap not far above the star's magnetic pole with a center-of-mass redshift because of the fall back's higher velocity and density. We expect that there are many such returning blobs at any one time, so observations repeated at the same phase will see the same level of emission. The projected area of the shock viewed by the observer, and hence the recorded emission of the resonance lines, would become maximum at $\phi = 0$. (The reverse would be the case at $\phi = 0.5$ when the project area of the cap would be minimal.) Clearly, this picture begs to be confirmed by MHD simulations of the type conducted for other Bp stars having stronger fields.

The putative auroral shock regions are represented as shaded regions at the "11 o'clock" and "5 o'clock" positions relative to the star in Fig. 4. In this new configuration at $\phi = 0$ these shocks have smaller areas but are denser than the the wind-shock interfaces discussed by Babel and SG01. Note that because the emissions and absorptions are formed mainly in two different regions of the magnetosphere, their volumes and column densities need not be equal. In addition, one expects that the UV line emission is formed in a separate region of the magnetosphere from the X-ray emissions. The energies released at the auroral caps can be expected to be moderate at most.

This picture suggests that sometimes one might see *small* amounts of blueshifted emission from the opposite hemisphere. As shown by Fig. 4, right panel, "4–5 o'clock" auroral cap contribution from the aurora over the opposing figure would exhibit a much smaller Doppler shift and projected area than the opposing cap. We can speculate that the very high microturbulence taken for conditions in a single structure in our previous models, are the result of a superposition in velocity of these two shocks (each with a smaller ξ).

5. Summary

Our modeling of the resonance line variations of ζ Cas shows that the disk occults the star to some degree during the entire rotation cycle. This attribute has not been found in the quantitative

modeling of other magnetic Bp stars whose lines we have examined (e.g., SG01, Smith 2003; Smith & Fullerton 2005, S06). It is probably more easily found for ζ Cas because of its small inclination angle i. In this geometry the disk occultation never realizes the full possible range of areal coverages (0–100%).

As mentioned, the large areal coverage factor found for our solutions at both $\phi = 0.0$ and 0.50 requires that the disk either extend nearly to the star's surface, extend to large distances from the central magnetic plane, or both. In Fig. 4, we noted that most or all the lines of sight to the star intersect the disk and thus suffer flux attenuation.

Consideration of the characteristics of the emission components in ζ Cas and the "classical" Bp stars shows that they cannot be easily understood with the kinematic description adopted by SG01, whether the emission arises from a shock at the edge of a cylindical or torus shaped disk. For example, for the Bp stars with dense or extensive disks investigated by SG01, the emissions can be present at all phases, and in all cases with a net redshift. We conjectured that this might be understood by shocks created by the collisions of dense fall back (blobs) with the outflowing wind. This releases the magnetic disk model from other interpretational inconsistencies. These include the frequent inequalities between the derived volumes in which the absorptions and emission are formed. It also addresses the high microturbulent velocities that are otherwise necessary to fit the line profile variations.

The analysis of lines of a modestly inclined system like ζ Cas clarifies these problems and provides cause for a reconsideration of the disk and emission region geometries. This shows that a final picture of these complicated star-disk system requires observations not merely over all viewing angles but of a sample of stars with a variety of rotational and magnetic inclination angles.

Acknowledgements. We thank the referee, Dr. Marc Gagné, for a number of comments that have added to the quality of this paper.

References

Babel, J., & Montmerle, T. 1997a, A&A, 323, 121
Babel, J., & Montmerle, T. 1997b, A&A, 485, L29
Gagné, M., Oksala, M. E., Cohen, D. H., et al. 2005, ApJ, 628, 986 (G05)
Grady, C. A., Bjorkman, K. S., & Snow, T. P. 1987, ApJ, 320, 376
Groote, D., & Hunger, K. 1976, A&A, 52, 303
Groote, D., & Schmitt, J. H. M. M. 2004, A&A, 418, 235
Neiner, C., Geers, V. C., Henrichs, H. F., et al. 2003, A&A, 411, 565 (N03)
Owocki, S. P., & Townsend, R. H. D. 2005, MNRAS, 357, 251
Preuss, O., Schussler, M., Holzwarth, V., et al. 2004, A&A, 417, 987
Sadsaoud, H., Le Contel, J. M., Chapellier, E., et al. 1994, A&A, 287, 509
Shore, S. A. 1987, AJ, 94, 731
Shore, S. A., & Brown, D. N. 1990, ApJ, 365, 665
Slettebak, A. 1994, ApJS, 94, 163
Smith, M. A. 2003, International Confrence on Magnetic Fields in O, B and A Stars, ed. L. Balona, H. Henrichs, & R. Medupe, ASP Conf. Ser., 305, 310
Smith, M. A. 2006, A&A, 459, 215
Smith, M. A., & Groote, D. 2001, A&A, 372, 208 (SG01)
Smith, M. A., Wade, G., Bohlender, D. A., et al. 2006, A&A, 458, 581 (S06)
Snow, T. P., Jr. 1981, ApJ, 251, 139
Sonneborn, G., Garhart, M., & Grady, C. 1987, in Physics of Be Stars, ed. A. Slettebak, & T. P. Snow., IAU Coll., 92, 286 (Cambridge Univ. Press)
Stellingwerf, R. F. 1978, ApJ, 224, 953
Tonneson, S. K, Cohen, D. H., Owocki, S. P., et al. 2002, BAAS, 201, #113.01
Townsend, R. H. D., & Owocki, S. P. 2005, MNRAS, 357, 251
ud-Doula, A., & Owocki, S. P. 2002, ApJ, 576, 413 (uO02)
ud-Doula, A., Townsend, R. H. D., & Owocki, S. P. 2006, ApJ, 640, L191 (u06)